

A Novel Technique of Rapid Solidification Net-Form Materials Synthesis

Melissa Orme

A novel method of net-form materials synthesis that is related to spray forming has been conceived, and initial verification experiments have been successfully completed. The method uses streams of ultra-uniform droplets of molten metal that are deposited onto a substrate in a controlled environment. The droplets are directed onto the substrate with measured angular dispersions as small as 2×10^{-6} radians, and speed dispersions as small as 3.5×10^{-7} times the average speed of the droplet, thereby facilitating the synthesis of small, detailed parts as well as large bulk parts with high resolution and a uniformly fine grain structure.

Keywords

processing, net shape forming, spray forming

1. Introduction

RECENT technical efforts and financial investment^[1-5] have been aimed at developing methods of net-form manufacturing that use rapid solidification. This is an important area of research investment for two reasons. First, net-form manufacturing should result in significant economic benefits because the product is made in one integrated operation, and second, rapid solidification leads to the well-known metallurgical advantages of small grain size, low segregation, low porosity, and increased homogeneity. Current state-of-the-art technology, which adopts the coupling of rapid solidification with net-form manufacturing, is a process termed "spray forming" in which a molten metal column is converted into a spray of droplets that is deposited onto a substrate where the particles undergo rapid solidification. Spray forming exploits the advantages of rapid solidification; however, its use is usually limited by the following considerations: (1) background pressures and gases surrounding the deposition process are fixed (by the atomization process), (2) the angle of the spray cone defines the resolution of the net-shaped part so that the fabrication of fine detailed features is prohibited without further machining, and (3) the droplets within the spray have a distribution of sizes and speeds that could lead to presolidified particles embedded within the deposit. Despite these limitations, spray forming has been shown to yield materials with enhanced mechanical properties over conventionally fabricated^[1,3,6] materials. This article describes the development of a new process in which the aforementioned limitations are overcome while the advantages are maintained, if not enhanced.

The new net-form process is characterized by the use of highly uniform droplet streams (each droplet of the order of 100 μm in diameter) as the deposition element. Recent research has led to a new technique of generating streams of drops in a vacuum environment that are more uniform and more controllable than those generated with any other conventional

method.^[7-9] Droplet speed variations as small as 3.5×10^{-7} times the average droplet speed can be achieved easily using the new technique, as verified by Orme et al.^[8] A molten metal droplet stream is illustrated in Fig. 1. Other droplet stream configurations, where the spacing and the size of each droplet in the stream are varied in a predictable and controllable manner, can also be achieved by using the methods described by Orme.^[9] Figure 2 illustrates four different droplet stream configurations that are generated with one nozzle, a fixed droplet speed, and a fixed droplet fluid. Each trace represents an independent droplet stream in which the peaks represent the droplets and the spacing between the peaks represents the spacing between droplets. The experimental traces were obtained with an optical probe technique, which is described in detail in Ref 8. The ability to manipulate the droplet stream configuration while maintaining (actually increasing, see Ref 9) the uniformity of the droplet speeds is a novel feature of the net-form manufacturing technique and is described in more detail in Section 3.1. This newly discovered ability of droplet control, combined with the advent of new developments in net-form manufacturing and rapid solidification, led to the concept of precision droplet stream manufacturing (PDSM), as described below.

1.1 PDSM: The Union of Droplet Stream Control and Net-Form Materials Synthesis

The union of the disciplines of net-form manufacturing and precise droplet stream control is the basis of precision droplet stream manufacturing.^[10] This technique relies on the use of

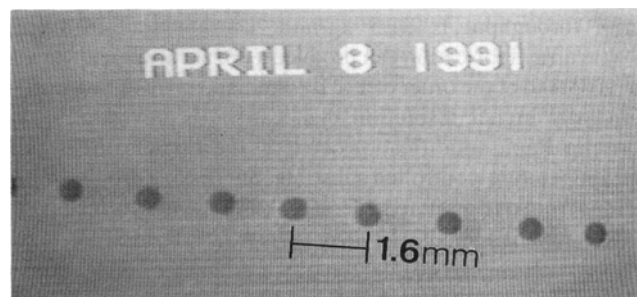


Fig. 1 Photograph of a molten metal droplet stream.

M.E. Orme, University of Southern California, Department of Aerospace Engineering, Los Angeles, CA 90089-1191.

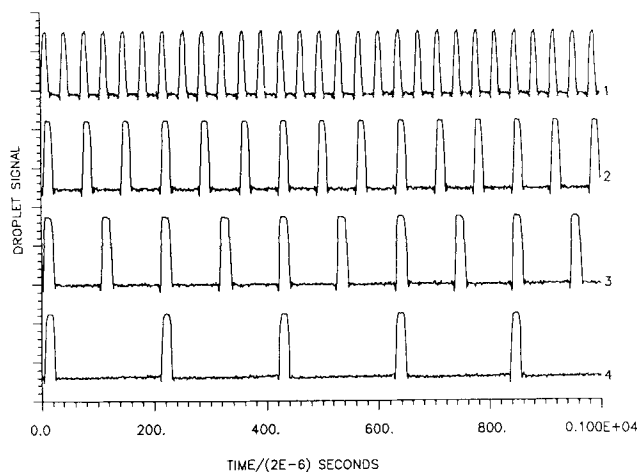


Fig. 2 Droplet configurations resulting from an amplitude-modulated disturbance with $N = 1, 2, 3$, and 6 . Peaks represent the droplets, and the time between peaks represents the time between droplets. The abscissa is the time of droplet passage normalized by the digitizing sampling rate (time/2 μ s, i.e., each division demarcates 40 μ s).

highly uniform streams of droplets by using the droplet generation methods described in Section 3.1. In operation, uniform droplets are directed onto a temperature-controlled substrate and undergo rapid solidification. The droplet deposition frequency, speed, size, and trajectory (impact location) are parameters that are predictable and flexibly controlled, which sets PDSM apart from spray forming. Equally important is the fact that the droplet generation and subsequent propagation can take place either in a vacuum environment to fabricate a net-form free of embedded gases or in a regulated inert or chemically active atmosphere to control the properties of the solidified material. This is possible because the droplet generation process is completely decoupled from the deposition environment. Molten metal is delivered to the droplet stream generators where droplets are formed due to capillary stream breakup.

To fabricate large parts, nozzle arrays are placed in the droplet generator to produce parallel streams of droplets. The arrays may have several hundred nozzles in each generator, with a separation of five to ten nozzle diameters for maximum material throughput. Nozzle array generators have been fabricated and tested.^[11] For an array of 300 streams, with typical dimensions of 150 μ m in diameter and stream speed of 5 m/s, the material throughput is 31.5 kg/min. Current state-of-the-art nozzle array fabrication can produce a nozzle array with an angular spread of the order of 1×10^{-3} radian,^[12] resulting in significantly higher resolution than can be achieved in spray forming. Rapid solidification occurs as the droplets impinge on the temperature-controlled substrate. Successive droplet depositions from one or more generators build the net-formed part.

To fabricate small, detailed parts, the nozzle array is replaced with a single nozzle, thereby producing a single droplet stream. Uniform molten metal droplets are directed by robotic arms onto the deposit. Rapid solidification occurs as each droplet arrives at the substrate. Successive droplet depositions build

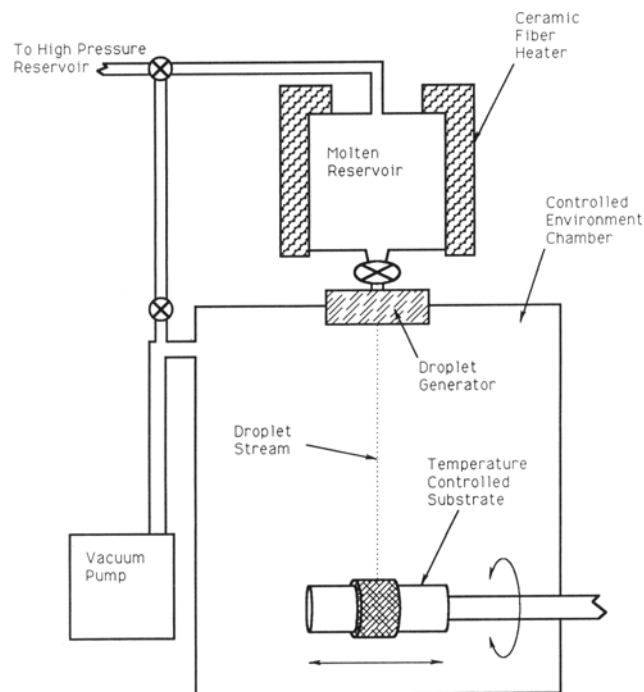


Fig. 3 Schematic of experimental apparatus.

the net-formed part. In this case, the material flow rate is 1.46 g/min. Because the angular spread of a stream of liquid droplets is on the order of 1×10^{-6} radians (illustrated in Ref 11), the resolution of the part is limited by the size of the droplet deformation upon impact. For droplet diameters for use with PDSM (25 to 150 μ m), the expected resolution of an edge of the net-formed part is expected to range from 12 to 150 μ m, which is a fraction of the splat diameter (see Section 3.3). This resolution is estimated by the splat diameter and the deposition scheme. The surface roughness of the net-formed part can be assumed to have a maximum value of the splat thickness, or a range of 2.2 to 2.8 μ m for the droplet diameters mentioned above. Thus, the projected resolution is comparable to, if not better than, the resolution that is achieved with typical machining processes, possibly making PDSM a true net-form process.

Once the droplets impinge on the previously deposited surface, they undergo rapid solidification. Rapid solidification causes the deposit to have a uniform structure that is virtually free of macrosegregation. Also, it is conceivable that the PDSM technique can be used to produce alloys that are impossible to manufacture with conventional manufacturing techniques because of shortcomings arising from fluid segregation. This can be done by supplying two or more independent generators with different materials and controlling the deposition rates of the relative materials.

2. Initial Experimental Results

Rose's metal was used as the droplet fluid, because it has a low melting point (≈ 460 K). Rose's metal is 50% bismuth, 27.1% lead, and 22.9% tin and has a specific gravity of 9.80. Its

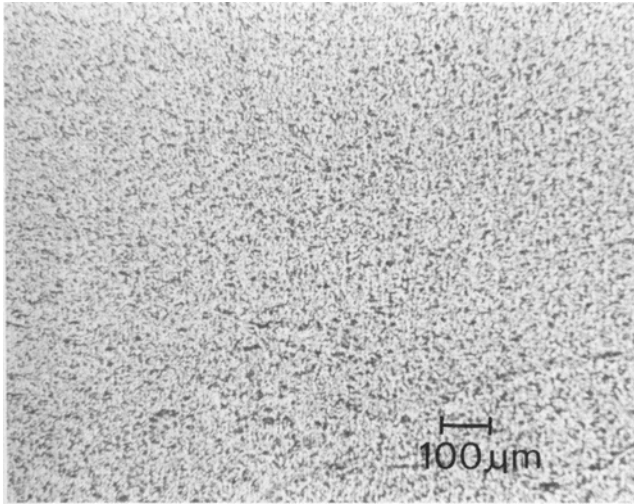


Fig. 4 Microstructure of Rose's metal when fabricated with controlled molten metal droplets.

surface tension (ζ) is 0.375 kg/s^2 . In the following calculations, values of thermal conductivity (κ), heat of fusion (l), specific heat (C), and thermal diffusivity (α) of $80 \text{ W/m}\cdot\text{K}$, $5.184 \times 10^4 \text{ J/kg}$, $122 \text{ J/kg}\cdot\text{K}$, and $6.89 \times 10^{-5} \text{ m}^2/\text{s}$, respectively, are used.

A schematic of the experimental apparatus is illustrated in Fig. 3. The main component is an 8-in. diam pyrex flight tube that is evacuated to background pressures typically on the order of 1×10^{-5} torr. A droplet generator is mounted to the top of the tube. The substrate, which takes the form of a pipe, was mounted in the chamber. The substrate is rotated about its long axis by a single-speed motor and is translated in the direction of its long axis. The substrate was chosen to have the shape of a pipe for convenience, but in practice it may be a variety of forms (an x - y table for instance).

Several pipe sections were deposited, and their microstructures were examined. Figure 4 illustrates the microstructure of the pipe section fabricated with controlled molten metal droplets. The grains are approximately uniformly sized, and the three phases of Rose's metal are approximately uniformly distributed. Figure 5 illustrates the microstructure of Rose's metal when fabricated with conventional casting. In the cast structure, coarse dendritic structures are visible, and thus, there is more segregation. Comparison of Fig. 4 and 5 demonstrates that the new method under development that involves the use of highly controlled molten metal droplets results in microstructure refinement.

The result shown in Fig. 4 is viewed as a baseline result, and with further development, the microstructure is expected to undergo further refinement. This is because the samples were made with a relatively crude substrate motion system that was unable to translate rapidly enough to ensure that successive droplet depositions had minimal overlap. As a result, the molten layer was several splats thick, leading to slower cooling rates and thus to larger grain structures. Future work involves the use of a higher speed positioning device.

The aforementioned angular dispersion of the droplet stream of a few microradians (illustrated pictorially in Ref 11)

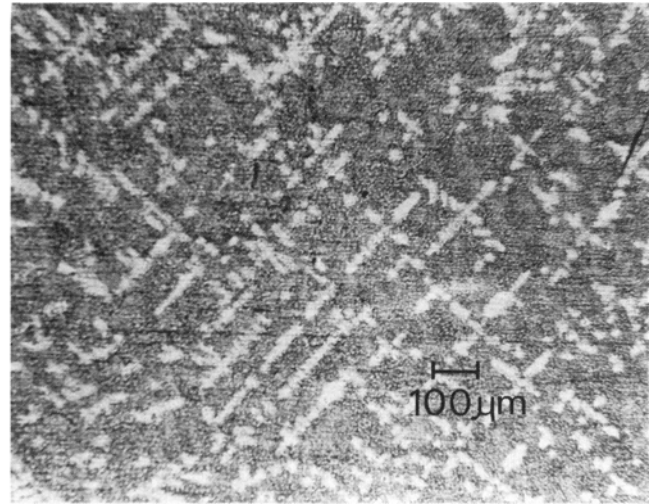


Fig. 5 Microstructure of Rose's metal when fabricated with conventional casting technique.

is the basis for the claims of the net-form manufacturing capability. To demonstrate this capability, the motion of the receiver (substrate) must move with an accuracy on the same order of magnitude as the droplets that are delivered. The initial experiments were obtained with a receiver system whose motion was too coarse to demonstrate the net-form capabilities of the technique. Further work is directed at achieving a tangible demonstration of the net-form capabilities that have been suggested. Section 3.3 illustrates important technical details that are relevant to achieving net-formed parts with tolerances equal to or better than those achieved with typical machining processes.

3. Technical Issues Relevant to Structural Integrity

3.1 Droplet Stream Control

Recent research has led to the precise control of droplet stream generation. Precise control refers to the ability to generate a stream of droplets with speed differences as small as 3.5×10^{-7} times the average droplet velocity^[8] and angular deviations of the stream of typically a few microradians.^[11] Furthermore, precise control refers to the ability to manipulate the configuration of the stream of droplets by adjusting an input disturbance to the droplet generator. It has been found that the fluid stream from which droplets are formed responds to the applied disturbance almost instantaneously (on the order of one disturbance wavelength). This means that a stream of droplets can be generated with droplets that are either very uniform (3.5×10^{-7} times the average droplet velocity) or that have a predictable and highly controllable size and spacing distribution.

3.1.1 Capillary Stream Breakup: General Phenomenon

Typically, the controlled instability of a fluid stream is introduced by vibrating the stream with a sinusoidal waveform. For the purposes of this article, an axisymmetric jet emanating from a nozzle of radius r_0 is considered. The stream travels at a

speed V_o , which is much greater than the capillary wave speed V_c and is perturbed with a periodic disturbance of wavelength λ . Rayleigh^[13] found that the disturbance on the stream will be unstable and cause droplet breakup if the wavelength of the disturbance is greater than the stream circumference. That is, if the nondimensional wavenumber k_o^* , given by $2\pi r_o/\lambda$, is less than one. He showed that the surface waves grow exponentially in time as $e^{\beta t}$, where β was given by Weber^[14] in a subsequent study:

$$\beta^2 + \frac{3vk_o^{*2}}{r_o^2}\beta = \frac{\zeta}{2\rho r_o^3}(1 - k_o^{*2})k_o^{*2} + \frac{V_o\hat{\rho}k_o^{*2}K_o(k_o^*)}{2r_o^2\rho K_1(k_o^*)} \quad [1]$$

where K_n is the n th order modified Bessel function of the second kind; ρ is the density of the fluid; $\hat{\rho}$ is the density of the ambient fluid; ζ is surface tension; and v is the kinematic viscosity of the fluid.

In a laboratory vacuum environment with a background pressure of 1×10^{-5} torr, the number density is approximately $3 \times 10^{11}/\text{cm}^3$, giving $\hat{\rho} \approx 7 \times 10^{-11} \text{ g/cm}^3$. At k_o^* values relevant to this study, the last term on the right side of Eq 1 is negligible. At background pressures of 1 atm or higher, this term is significant, and the resulting wave growth leading to stream breakup is shown to be affected by aerodynamics.^[15,16]

It has been observed that the droplets have a random speed dispersion, which has been suggested to originate when the stream breaks to form a droplet.^[8,17] The magnitude of the dispersion can be reduced by an order of magnitude by applying a new form of disturbance to the stream.^[7,8]

3.1.2 New Method of Capillary Stream Breakup

The droplet breakup process described in the previous section is referred to as “conventional” droplet breakup, because a sinusoidal disturbance is conventionally applied to the stream, which results in a stream of droplets that are separated a center-to-center distance of the wavelength of disturbance. New droplet stream configurations that have different separations than those achieved with conventional droplet breakup can be achieved if the stream is perturbed with an amplitude-modulated disturbance. It has been noted that the capillary stream essentially “mimics” the general features of the applied disturbance, so that knowledge of the response of the stream to the disturbance allows the predictable and flexible generation of droplets at precisely controlled time intervals. For example, if the conventional sinusoidal disturbance (“carrier” disturbance) is modulated with a disturbance whose frequency is an even divisor of the carrier frequency, the resulting stream of droplets, which are called “modulation” drops, are separated by the long, or modulation, wavelength. If the frequency ratio N is defined as the ratio of the carrier to the modulation frequencies, the separation of the modulation drops are N times the carrier separation. This is shown in Fig. 2, in which the first trace is the analog representation of the carrier droplets, and the second through fourth droplet traces were achieved by applying a modulation such that the frequency ratio is 2, 3, and 6, respectively. The mass of the modulation drop is N times that of the carrier droplet, or it can be said that each modulation drop

contains N carriers. Furthermore, it has been shown that if the uniformity of the carrier drops is σ_c , the speed uniformity of the resulting droplets upon applying a modulation to the disturbance (such that N is an integer) is $\sigma_m = \sigma_c/N$.^[8] A description and model of the physical phenomenon that occurs when disturbing the stream with an amplitude-modulated disturbance is given by Orme et al.^[8]

The structure of the net-formed product depends primarily on the solidification characteristics of the droplets. Parameters that affect the solidification properties are the mass flow rates, deposition scheme, substrate temperature, and environment control. In the following sections, methods to obtain the net-formed part with the highest structural integrity are described.

3.2 Droplet Delivery Rate

It is desired to achieve a droplet delivery rate such that the molten droplets arriving at the previously deposited surface will arrive at a molten film only a few microns thick. Upon impact, the droplets will splat on the surface, causing the liquids to mix, thus removing the boundaries. Equiaxed grains grow within each splat until the next splat arrives. Because the surface on which the particles impinge is liquid, the splatting action may cause many of the dendritic arms to break. Control of the droplet delivery rate is achieved through coupled manipulations of droplet speed, nozzle size (coupled through the Rayleigh condition for droplet production as discussed in Section 3.1), and substrate motion speed.

3.3 Deposition Schemes and Net-Form Accuracy

It was stated previously that nozzle diameters in the range of 25 to 150 μm are suited for this process. For the droplet generation parameters of stream speed, fluid density, surface tension, and nondimensional wavenumber equal to 5 m/s, 9800 kg/m^3 , 0.375 kg/s^2 , and 0.697, respectively, a 25- μm nozzle results in a 47- μm droplet and a 150- μm nozzle results in a 283- μm droplet. The 47- μm diameter droplets will be delivered at a rate equal to 44.3 kHz if no modulation is used and will have a center-to-center separation equal to 113 μm . The 283- μm droplets will be generated at a frequency of 7.4 kHz and will have a center-to-center separation equal to 695 μm . Thus, deposition rates ranging from 1.46 g/min for the 25- μm nozzle to 105 g/min for the 150- μm nozzle can be obtained.

There is a multitude of droplet deposition schemes that can be identified for use with the PDMS technique. The usefulness of the different schemes will depend on the shape of the part made and the desired material characteristics. Figure 6 illustrates two possible deposition schemes, as viewed from above. The resolution of the net-formed part depends on the deposition scheme used. Figure 6(a) illustrates the top view of a layer of splats on a substrate. Droplets are delivered so that the splats overlap as shown, minimizing the porosity of the material. As each splat is delivered, its boundaries will become smeared with the neighboring molten mass from neighboring splats. Each layer of the deposit will consist of a matrix of splats. The edge resolution of the material, Δ , is indicated by arrows on the figure. In Fig. 6(a), it is easy to see that the resolution is $D/2$, where D is the splat diameter. The delivery of the subsequent layer can be offset, as shown in Fig. 6(b), and must be pro-

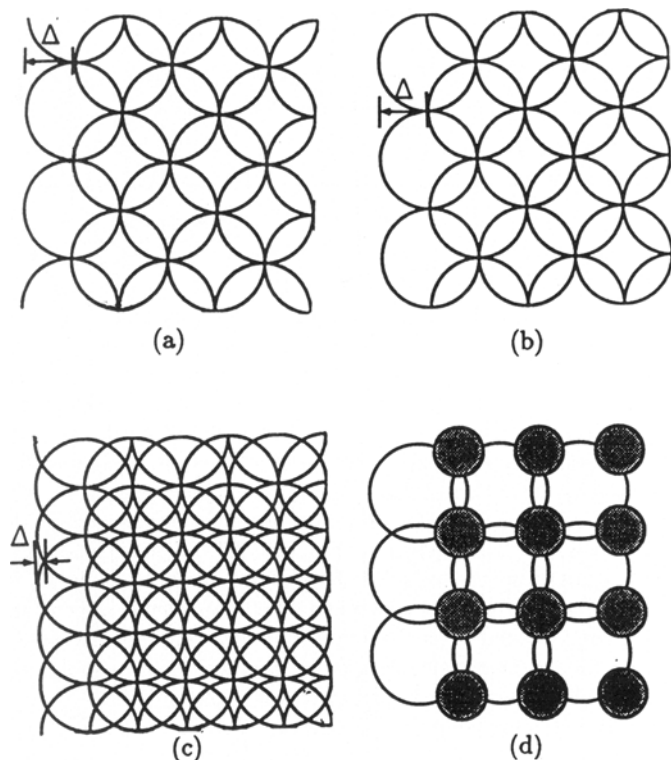


Fig. 6 Examples of splat deposition schemes as viewed from above. (a) First layer of deposit matrix. (b) Second layer. (c) Superimposed layers. (d) Deposition scheme using two different sized splats.

grammed so that the previous layer is not completely solidified, allowing mixing and elimination of splat boundaries. An idealized view of the superposition of the two layers is shown in Fig. 6(c). By geometric considerations, the fabrication resolution, Δ , of the two-layer part made with the scheme illustrated in Fig. 6(c) is $\Delta = D \left(\frac{1}{2} - \frac{\sqrt{3}}{4} \right) = 0.067D$. Deposition of additional layers will reduce the resolution if the appropriate offset is used.

Based on previous research directed at studying the controlled collisions of droplet streams in a vacuum, the droplets described above will spread to disks that are 178 μm (from the 25- μm nozzle) and 2.29 mm (from the 150- μm nozzle).^[18]

Thus, for the splats with $D = 2.29$ mm and $D = 178$ μm , the edge resolutions of the net-formed parts are $\Delta = 153$ μm and $\Delta = 12$ μm , respectively. The resolution can be reduced further by offsetting the splats in subsequent layers at values different from those shown in Fig. 6(a) and (b). Because the droplet streams have angular dispersions that are typically a few times 1×10^{-6} radians, a transit distance of 0.5 m from the droplet generator to the substrate, for example, results in the splat placement error associated with this dispersion of 1 μm (using an angular dispersion of 2×10^{-6} radians). Assuming that the accuracy of the positioning device moves with a similar accuracy, this provides an illustration of the necessity of using highly controllable droplet streams to synthesize net forms

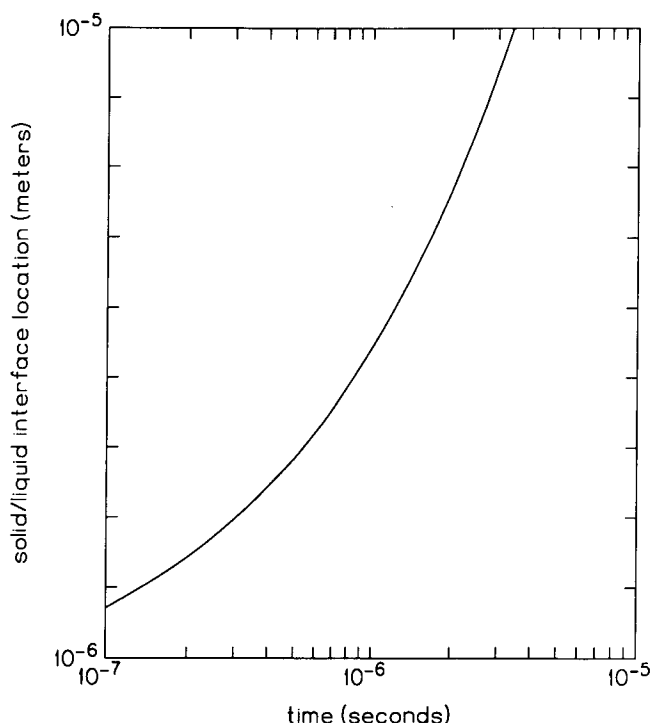


Fig. 7 Solid/liquid interface location during phase change of a 10- μm thick splat of over-heated Rose's metal (overheated by 50 $^{\circ}\text{C}$) when deposited onto a cooled substrate of 40 $^{\circ}\text{C}$ at time $t = 0$.

with very fine tolerances. Figure 6(d) is an example of how two differently sized droplets may be used to fill in the interstices between droplets. The differently sized droplets may be directed from different generators, or from the same nozzle by generating droplet patterns (predictable patterns of differently sized and separated droplets) with the method described in Ref 9. Also, more than one type of molten metal can be used to make in situ alloys.

3.4 Heat Transfer Considerations

It is well known that many of the structural features that ultimately control product properties are set during solidification. Solidification occurs in two stages: nucleation and growth. Nucleation generally occurs when the melt is super-cooled. Thus, it is necessary that the temperature of the molten metal be lower than or equal to its melting point when it makes contact with the substrate. The second step in the solidification process is growth, which occurs as the heat of fusion is continually extracted from the liquid. The direction, rate, and type of growth can be controlled by how heat is removed from the liquid.

3.4.1 Preliminary Model of Deposition and Solidification

The control of the heat transfer from the molten metal drop to the substrate is one of the most important control parameters that regulate the structural integrity of the net-formed material. This is because the solidification rate determines the grain size

of the material, which in turn determines its mechanical characteristics. A model of the solidification characteristics coupled with the deposition schemes is essential to guide the experiments. Variables of the model are the droplet diameter d_o , Weber number, W_e , droplet production rate, f , and the deposition scheme. From the above variables, the splat diameter D and thickness h are determined from the results of Cheng^[19] or the results of Muntz et al.^[18]

In an initial attempt to estimate the time required to cool a splat of thickness h , originally at its melting temperature T_m and suddenly exposed to the substrate at temperature $T_s < T_m$ located at $y = 0$, several assumptions are made. First, undercooling is neglected. Second, it is assumed that the heat liberated by the phase change is removed by conduction (convection and radiation are neglected). Third, it is assumed that the phase change occurs at a specific temperature (i.e., $T_{\text{liquid}} = T_{\text{solid}} = T_{\text{melt}}$ at the solid/liquid interface). Finally, it is assumed that the material properties are equal in both the liquid and solid phase. The temperature is governed by the unsteady one-dimensional heat conduction equation:

$$\frac{\delta T_j}{\delta t} = \frac{\delta}{\delta y} \left(\alpha_j \frac{\delta T_j}{\delta y} \right) \quad [2]$$

where α is the thermal diffusivity; the subscript j represents either liquid or solid; y is the vertical coordinate (normal to the substrate surface); and T is the temperature.

Neumann's solution is used as outlined by Özisik.^[20] A plot of the solid/liquid interface location during the phase change of a 10- μm thick splat of Rose's metal is shown in Fig. 7. It can be seen that the splat will solidify in approximately 3×10^{-6} s. Based on the work of Cheng,^[19] the solidification time is on the same order as the time required for a droplet to spread. Thus, a more detailed analysis of the dynamics of the spreading of a drop coupled with the transient heat conduction is required to realistically model the droplet deposition and solidification process.

As the net-form thickness grows by the deposition of several layers of splats, the cooling properties change. The temperature of the substrate must be controlled to accommodate for the additional thickness, L . To estimate the change in temperature required, the heat flux arriving at the deposit is equated to the heat flux removed by the substrate, where the heat flux arriving is assumed to be dominated by heat of fusion because the deposition temperature is near the solidification temperature. The temperature of the substrate can be estimated as:

$$T_s = T_m - \frac{f \rho h L (L + h)}{\kappa} \quad [3]$$

where κ is the thermal conductivity. Table 1 illustrates the reduction in substrate temperature that is required to accommodate the increasing thickness (L) of the deposit. This formulation is a steady-state approximation of what is, in reality, an unsteady problem. It is unsteady because the material response to the temperature reduction of the substrate is not instantaneous.

Table 1 Temperature drop as a function of deposit thickness

Deposit thickness, L	T_s, K
100 μm	453
500 μm	429
1 mm	397
5 mm	151

3.5 Environmental Control

The extent of the destructive effects of the ambient environment on the net-formed material depends on the deposition rate. For example, if the droplet density (number of droplets per unit volume) is low and if the environment is rich with oxygen, then oxygen from the ambient environment will settle on each splat boundary leaving a thin oxide film. The thin impurity film may also be formed from contamination in the liquid metal. This occurs because many impurities such as oxygen are capable of being dissolved in the liquid metal. However, they are often not soluble in the solid phase of the metal. When the metal freezes, the impurities remain in the liquid. Thus, impurities are concentrated in the final liquid film that has not solidified. This layer prevents surface wetting, and the resulting structure has well-defined splat boundaries as well as porosity.

The effect of impurities is less destructive if the mass flow rate is high. This is because the droplets will impinge on a liquid surface, and the boundaries will be obliterated. As the liquid solidifies, the impurities will rise to the top where the material is still in the liquid form. If the flow rate is sufficiently high, yet not so high as to lose the benefits associated with rapid solidification, the final structure can be one of low porosity and fine grain size, with a film of impurities concentrated on the top layer. Manufacturing in a pure vacuum environment will alleviate the damaging effects of oxidation. However, there may be other impurities present that are soluble in the liquid metal, as well as insoluble impurities such as sand and slag. If impurities are present in the manufacturing environment of PDSM, new methods must be developed to minimize their effects.

4. Summary

A new technique of net-form manufacturing has been described. The method uses highly controllable streams of molten metal droplets as the deposition element, which undergo rapid solidification as they impinge on a temperature-controlled substrate. Control of the droplet stream trajectories to a few microradians may allow precise deposition and material buildup with high resolution. Control of the droplet speeds to 3.5×10^{-7} times the average droplet speed allows uniform cooling and thus uniform material characteristics, e.g., small and uniform and fine grain size, low porosity, homogeneity, and no macrosegregation, all of which lead to a material with high structural integrity. Preliminary experimental results have been reported, and technical issues that are essential to achieve enhanced qualities have been described. On-going work includes time-dependent heat transfer modeling coupled with the dynamics of the spreading of a droplet to be used to guide carefully controlled experiments. It is suggested that this process

may alleviate many of the limitations associated with the closest existing technology of net-form manufacturing involving rapid solidification from the molten phase, while maintaining, if not improving, the metallurgical properties.

Acknowledgments

This research was funded in part by NSF grants CTS-8921922 and DDM-9204201 and by the USC FRIF award.

References

1. B.A. Rickinson, F.A. Kirk, and D.R.G. Davies, *Powder Metall.*, Vol 1, 1981, p 1
2. A.R.E. Singer, *Mater. Design*, Vol 4, 1983, p 892
3. R.W. Evans, A.G. Leatham, and R.G. Brooks, *Powder Metall.*, Vol 28, 1985, p 13
4. H.C. Fielder, T.F. Sawyer, R.W. Kopp, and A.G. Leatham, *JOM*, Vol 28, 1987
5. E.J. Lavernia, J.D. Ayers, and T.S. Srivatsan, *Int. Mater. Rev.*, Vol 37, 1992, p 1
6. M. Gupta, F. Mohamed, and E.J. Lavernia, *Metall. Trans. A*, Vol 23, 1992, p 831
7. M. Orme and E.P. Muntz, *Rev. Sci. Instrum.*, Vol 58, 1987, p 279
8. M. Orme and E.P. Muntz, *Phys. Fluids J. A*, Vol 2, 1990, p 1124
9. M. Orme, K. Willis, and V. Nguyen, *Phys. Fluids J. A*, Vol 5, 1993, p 80
10. M. Orme and E.P. Muntz, U.S. Patent 5,171,360, 1992
11. M. Orme, T. Farnham, G. Pham Van Diep, E.P. Muntz, and A. White, AIAA 22nd Thermophysics Conference, AIAA-87-1538, Honolulu, Hawaii, 1987
12. B. Stanley, E.I. DuPont De Nemours & Company, private communication, Mar 1988
13. Lord Rayleigh, *Proc. London Math Soc.*, Vol 10, 1879, p 4
14. C. Weber, Z. Agnew, *Math Mech.*, Vol 11, 1931, p 136
15. R.P. Grant and S. Middleman, *A.I.Ch.E. J.*, Vol 12, 1966, p 669
16. A.M. Sterling and C.A. Sleicher, *J. Fluid Mech.*, Vol 68, 1975, p 477
17. M. Orme, *Phys. Fluids J. A*, Vol 3, 1991, p 2936
18. E.P. Muntz, M. Orme, D. DeWitt, M. Wilson, F. Fusse, and M. Tansey, *Bull. Am. Phys. Soc.*, Vol 33, 1988, p 2241
19. L. Cheng, *Ind. Eng. Chem. Process Des. Dev.*, Vol 16, 1977, p 192
20. M.N. Özisik, *Heat Conduction*, John Wiley & Sons, 1980